Thermally induced inversion of Al-substituted titanomagnetite in basalts: Evidence for partial self-reversal

Yongxin Pan,[1] Qingsong Liu,[2] Chenglong Deng,[1] Huafeng Qin,[1] and Rixiang Zhu[1]

Received 16 June 2006; revised 1 September 2006; accepted 27 September 2006; published 29 November 2006.

[1] We report properties of laboratory-induced thermoremanence combined with detailed rock magnetic experiments on basaltic samples which contain aluminum-substituted titanomagnetite ($Fe_{2.24}Ti_{0.64}Al_{0.12}O_4$). Prior to Thellier-Coe paleointensity experiments, specimens were first demagnetized using an alternating field with a peak field of 90 mT and were then imparted an anhysteretic remanent magnetization (ARM) to represent a natural remanent magnetization (NRM). Results show that the partial thermal remanent magnetization (pTRM) gain and ARM remaining are linearly correlated up to 300°C. Between 300 and 460°C, specimens acquire thermoremanence with a direction antiparallel to the external field direction, leading to intensity decreases. This coincides with the onset of the mineral transformation from Al-titanomagnetite to a magnetic phase with higher T_c. Our results support that phase interaction with distinct T_c values in partially oxidized titanomagnetite can produce partial self-reversal thermoremanence in rocks.

Citation: Pan, Y., Q. Liu, C. Deng, H. Qin, and R. Zhu (2006), Thermally induced inversion of Al-substituted titanomagnetite in basalts: Evidence for partial self-reversal, *J. Geophys. Res.*, *111*, B12S29, doi:10.1029/2006JB004576.

1. Introduction

[2] Titanomagnetite ($Fe_{3-x}Ti_xO_4$, $0 \leq x \leq 1$) and their derivatives are ubiquitous in submarine and continental basalts, and are usually the dominant carriers of the corresponding natural remanent magnetization (NRM). In early paleomagnetism studies, there is an argument on the mechanism of the reversed NRM recorded in natural samples: authentic behavior of the paleomagnetic field or self-reversal of the thermal remanent magnetization (TRM) [*Verhoogen*, 1956]. *Néel* [1951] put forward two mechanisms for interpreting self-reversal of RM: the single-phase model and two interacting magnetic phase models. Alternatively, *Verhoogen* [1956] proposed that ionic reordering during low-temperature oxidation of titanomagnetite can also yield self-reversal of RM. However, it is rather experimentally difficult to reproduce this process in laboratory. Later, *O'Reilly and Banerjee* [1966] found that very high oxidation state and high temperature are prerequisites for self-reversal of RM. Self-reversal of TRM could also be caused by negative magnetic coupling [e.g., *Havard and Lewis*, 1965; *Tucker and O'Reilly*, 1980; *Heller and Petersen*, 1982; *Krása et al.*, 2005].

[3] Self-reversal of NRM has been documented in dacite (hemoilmenite as the dominant magnetic carrier), oxidized oceanic and continental basalts (titanomagnetite as the dominant magnetic carrier) with a wide range of ages from Neogene to Cretaceous ages [e.g., *Nagata et al.*, 1952; *Schult*, 1968; *Heller and Petersen*, 1982; *Hoffman*, 1982; *Bina et al.*, 1999; *Gapeev and Gribov*, 2002; *Doubrovine and Tarduno*, 2004]. It has also been shown that TRM produced under moderate- to high-temperature oxidation conditions in the laboratory can undergo self-reversal [e.g., *Havard and Lewis*, 1965; *Tucker and O'Reilly*, 1980]. This makes it feasible to determine under which conditions self-reversal of RM could occur and then to decipher the corresponding mechanisms that control the self-reversal processes. Recently, *Krása et al.* [2005] carried out comprehensive rock magnetic experiments and numerical modeling studies on continental basalts from Olby (France) and Vogelsberg (Germany). Their results revealed that partial and/or full self-reversal of RM in basalt are caused by phase coupling of two side-by-side phase assemblages with different blocking temperatures. They further found that partial oxidation of the grain does not only influence the Curie temperature (T_c) (hence the blocking temperature, T_b), but also the domain configuration. During acquisition of TRM, the magnetic coupling makes remanence carried by the lower T_c phase antiparallel to the applied external magnetic field. However, in these previous studies, full vector analysis of the self-reversal of TRM is lacking.

[4] In this paper we investigated the thermoremanence carried by basaltic samples that contain aluminum-substituted titanomagnetite (chemical composition $Fe_{2.24}Ti_{0.64}Al_{0.12}O_4$). First, we aim to detect the possibility of self-reversal of thermoremanence caused by laboratory thermal treatment. Second, we test the remanence stability and determine magnetomineralogical inversions during heating.

2. Samples

[5] The Neogene age Hannuoba basalts represent the most intensive Cenozoic volcanism in northern China.

[1] Paleomagnetism and Geochronology Laboratory (SKL-LE), Institute of Geology and Geophysics, Chinese Academy of Sciences, Beijing, China.
[2] National Oceanography Centre, University of Southampton, Southampton, UK.

0148-0227/06/2006JB004576$09.00

Table 1. Electron Microprobe Analysis Data From the Studied Hannuoba Alkalic Basalt Sample

	Individual Magnetic Mineral Particles						
Oxide	1	2	3	4	5	6	Average
SiO_2	0.0444	0.1133	0.0603	0.081	0.0735	0.0745	0.0745
TiO_2	21.3567	21.3671	20.3091	21.7338	23.6113	22.2915	21.7783
Al_2O_3	3.3838	3.3175	2.2964	2.5175	2.5891	1.5181	2.60373
Cr_2O_3	0.3819	0.1843	0.1353	0.1834	0	0.1091	0.16567
Fe_2O_3	23.8014	23.0919	26.4669	24.4916	20.379	23.0751	23.551
MgO	1.6091	1.2214	0.9697	1.3323	1.5794	0.98	1.28198
CaO	0.1277	0.3111	0.1643	0.2308	0.1298	0.2086	0.19538
MnO	0.662	0.5309	0.5461	0.6511	0.5107	0.7738	0.61243
FeO	48.1437	48.527	47.833	48.9327	50.1244	49.0626	48.7706
NiO	0	0.1438	0	0.1154	0.0064	0	0.04427
ZnO	0	0.2675	0.1439	0	0	0.1174	0.08813
Na_2O	0.003	0.0237	0.012	0.0089	0.0266	0.0239	0.01635
K_2O	0.0433	0.0185	0.0366	0.0524	0	0.0214	0.0287
Sum	99.557	99.118	98.974	100.331	99.030	98.256	99.211

Lithologically, they consist of alkalic and tholeiitic basalts [e.g., *Zhi et al.*, 1990; *Fan and Hooper*, 1991; *Chen et al.*, 2001]. Their K-Ar ages are between about 32 and 6 Ma [*Zheng et al.*, 2002; *Zhu et al.*, 2003; *Pan et al.*, 2005]. Earlier rock magnetic and paleomagnetic investigations revealed that partially oxidized Ti-rich titanomagnetite, which is characterized by low T_c ($\sim$150°C), is the major carrier of NRM [*Tian et al.*, 2002; *Pan et al.*, 2005]. Hannuoba alkalic basalt blocks collected from southern Inner Mongolia were used in the present study. Electron microprobe analysis of the opaque grains shows aluminum-substituted titanomagnetite (ATM), with a chemical composition of $Fe_{2.24}Ti_{0.64}Al_{0.12}O_4$ (see Table 1), in the size range of <20 μm. T_c of $\sim$100–150°C supports the presence of titanomagnetite with high titanium content (e.g., $x \sim 0.6–0.7$) [*Dunlop and Özdemir*, 1997], which is a typical phase of low-oxidized state in rapidly cooled basaltic lavas. The composition x estimated from the T_c is consistent with the Fe/Ti ratio determined by electron microprobe analysis.

[6] Light microscopy examinations on thin sections cut from various positions show nearly homogeneous lithologic properties for the whole block. Subsequently, eleven cubic specimens with 1-cm sides, named NLB-a to c and NLB-1 to 18, were cut for magnetic experiments. Three perpendicular orientation lines (x, y, z) were arbitrarily marked on the cubes for reference in measurements.

3. Thellier-Coe Experiment

[7] The Thellier-Coe paleointensity experiments [*Thellier and Thellier*, 1959; *Coe*, 1967] with sliding pTRM checks [*Prévot et al.*, 1985] on a set of fresh specimens (NLB-a to c) were carried out using a French paleointensity furnace (residual field <10 nT) installed in a magnetically shielded room (<300 nT). In order to avoid contaminations from NRM, all specimens were first demagnetized in an alternating field (AF) at 90 mT, followed by imprinting of anhysteretic remanent magnetization (ARM) in a peak AF field of 80 mT with a bias field of 50 μT along the designated $-z$ axes (except NLB-c, which was magnetized along the y axis). The ARM was regarded as the ''NRM'' in present study. ARM has long been regarded as a suitable analogue of TRM to avoid chemical alterations upon heating [*Thellier and Thellier*, 1959; *Banerjee and Mellema*, 1974; *Yu et al.*, 2003]. For ARM, as the AF field decays, the remanence is gradually blocked when the peak value of AF falls below the microscopic coercivity of magnetic grains in samples. This process resembles the TRM acquisition process that remanence is gradually frozen when cooling a sample through the T_b. *Yu et al.* [2003] showed that the TRM/ARM ratio is grain-size-dependent. Nevertheless, for single-domain (SD) and multidomain (MD) magnetic particles, the alternating field and thermal stabilities of ARM and TRM are very similar. An exception was observed for magnetite particles with a grain size of $\sim$240 nm, which could have a domain state very different from both SD and MD particles. However, our specimens contain much larger grain sizes (<20 μm). Therefore it is feasible to use the laboratory-induced ARM to mimic the natural TRM.

[8] Specimens were then stepwise heated to fifteen elevated temperatures at 50, 100, 150, 200, 250, 300, 330, 350, 380, 400, 430, 460, 500, 530, and 560°C. For each run, specimens were heated twice: in a zero field for the first heating and in an applied field of 30 μT along the *z axis* for the second heating. For the in-field treatment, the external field was applied during both heating and cooling cycles. When the treated temperature exceeded 200°C, a third in-field heating and cooling cycle was performed to a lower temperature for pTRM checks. To minimize effects of thermal lags, the heating rate was reduced at about 60°C below the required peak temperature, from 3.2°C/min down to 1°C/min, which was maintained until the peak temperature was attained (and then held for 30 minutes). Specimens were left to cool naturally overnight. Prior to each run, air was first evacuated from the furnace with a primary vacuum pump, then argon gas was flushed in and pumped out of the chamber at least three times. Argon gas was circulated gently through the furnace during the whole experimental process.

[9] Results show that pTRM increases up to 300°C, followed by a decrease up $\sim$400°C, and then it exhibits a slight increase above $\sim$450°C. In contrast, ARM is demagnetized rapidly to less than 20% below 200°C, followed by a slight increase between $\sim$300 and 400°C (Figures 1a and 1b). The pTRM checks show lower intensities than those of the previous pTRMs at the same temperatures. The corresponding Arai plots (Figures 1c and 1d) indicate a linear relationship between the ARM remaining and pTRM gain up to 300°C. The estimated field intensity is only one third of the external field intensity. This can be partially interpreted by the grain size dependence of ARM. *Yu et al.* [2003] showed that the best fit slope (or TRM/ARM ratio) from pseudo-Thellier experiments has a strong grain size dependence above 0.2 μm and it decreases with increasing grain size. Above 300°C, however, pTRM gain decreases, rather than increases.

[10] Figure 2 shows the orthographic projections of components x, y, and z of ARM and pTRM from the Thellier-Coe paleointensity experiments. The ARM (z components in NLB-a,b and y component in NLB-c) are gradually demagnetized with a significant remanence loss when the temperature reaches the $T_c \sim 100–150$°C; however, between 300 and 400°C, the z component remanences of these specimens peculiarly increase (see insets in Figures 2a–2c), which is followed by a further demagnetization. The pTRM (z components parallel to the external applied field) continuously gains below 300°C. However,

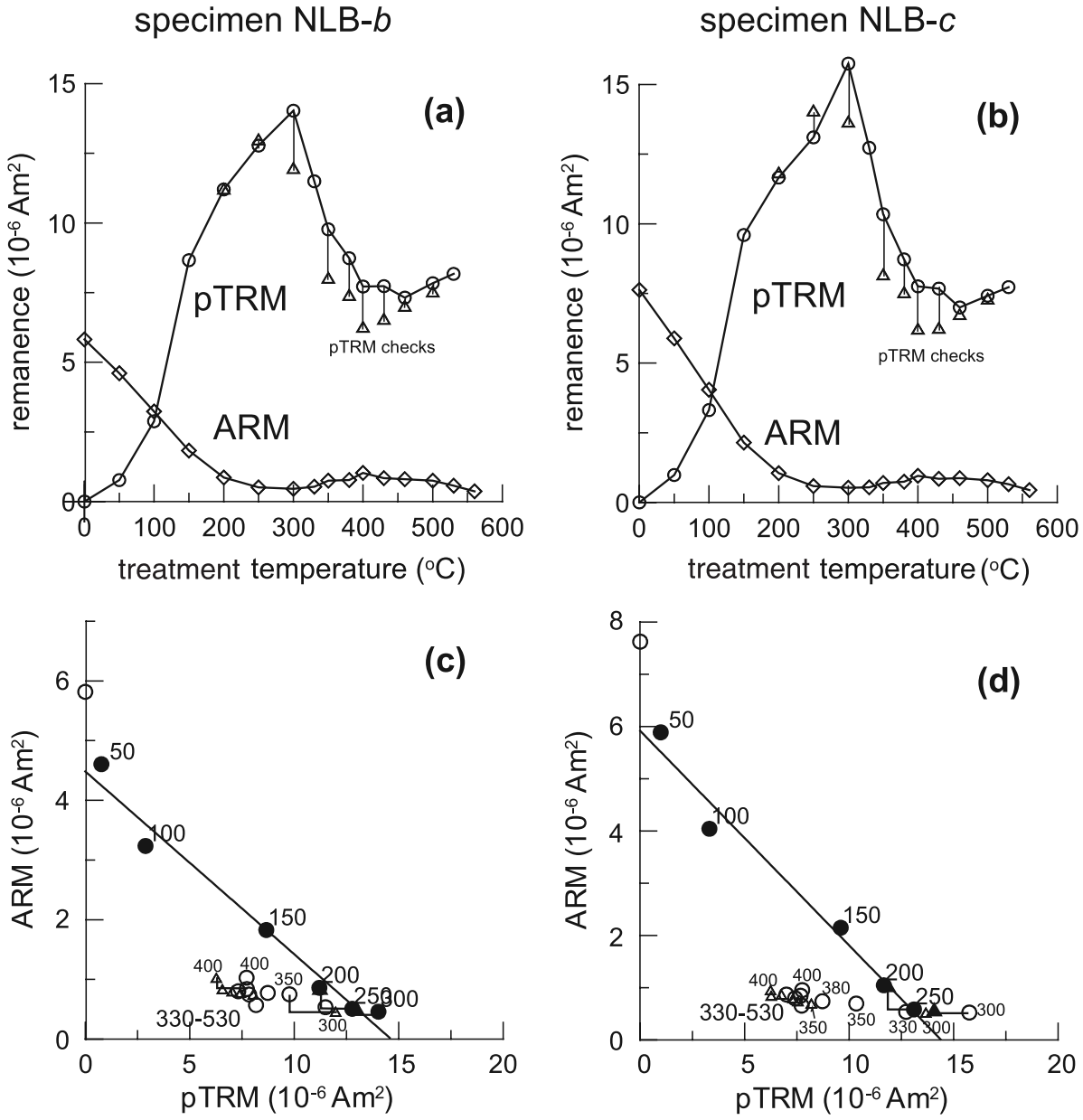

Figure 1. Partial TRM acquisition (applying an external field 30 μT during both heating and cooling) and demagnetization of a laboratory imparted anhysteretic remanent magnetization (ARM) (here taken as "NRM") and their Arai plots. The pTRM checks (triangles) are shown. In Figures 1c and 1d, solid (open) triangles and circles stand for positive (negative) pTRM checks and points used (not used) for intensity estimation, respectively.

between ~300 and 460°C a backward behavior is clearly observed in all specimens (Figures 2d–2f). This decrease in pTRM gains as well as negative pTRM checks shown in Figure 1 could be caused by either an offset of new components or destruction of a strongly magnetic phase. The latter is not supported by the relatively stable saturation remanence (M_{rs}) and magnetization (M_s) upon heating at this temperature interval (see below discussion).

4. Rock Magnetic Experiments

[11] We carried out a series of rock magnetic experiments on both fresh and thermally treated specimens to check for magnetomineralogical inversion, changes of domain states and magnetization capacities induced by laboratory heating.

4.1. Thermomagnetic Curves

[12] To test the thermal stability of ATM, we measured two types of thermomagnetic curves. The temperature dependence of low-field magnetic susceptibility (k–T) curves were stepwise heated in an argon atmosphere in fifteen steps up to 700°C using a Kappabridge KLY-3 equipped with a CS-3 temperature apparatus. The k–T curves are nearly reversible for 100, 150, 200 and 250°C runs, and the corresponding T_c is estimated to be ~100–150°C (Figure 3a). After heating to 300°C, the cooling curve is

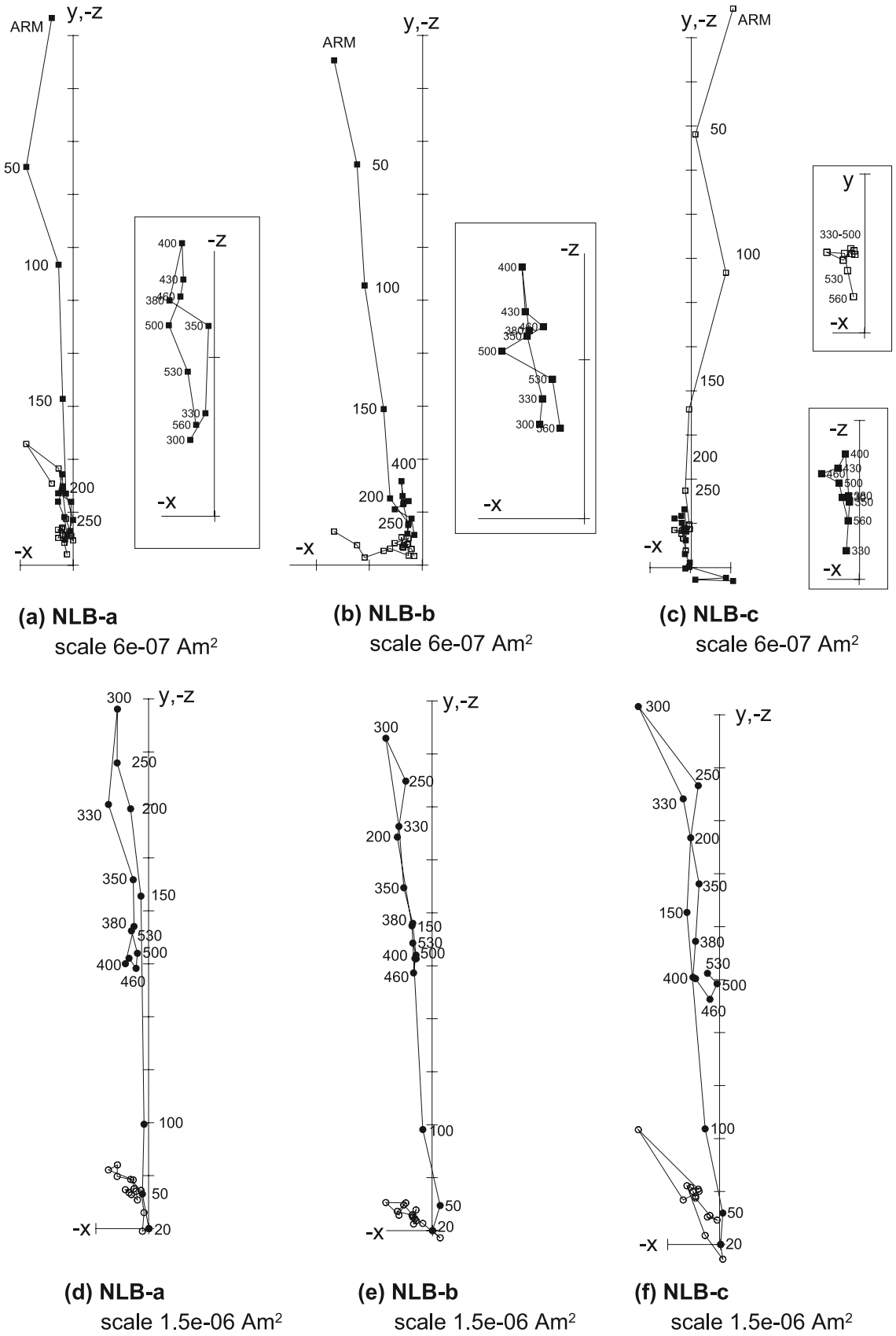

Figure 2. (a–c) Orthogonal projections of the demagnetization of "NRM" and (d–e) acquisition of pTRM in Thellier-Coe experiments. Note, in pTRM acquisition the laboratory field (30 μT) was parallel to the z axes of the specimens. Temperatures are shown in °C. Note that the "NRM" was imparted along the y axis for specimen NLB–c.

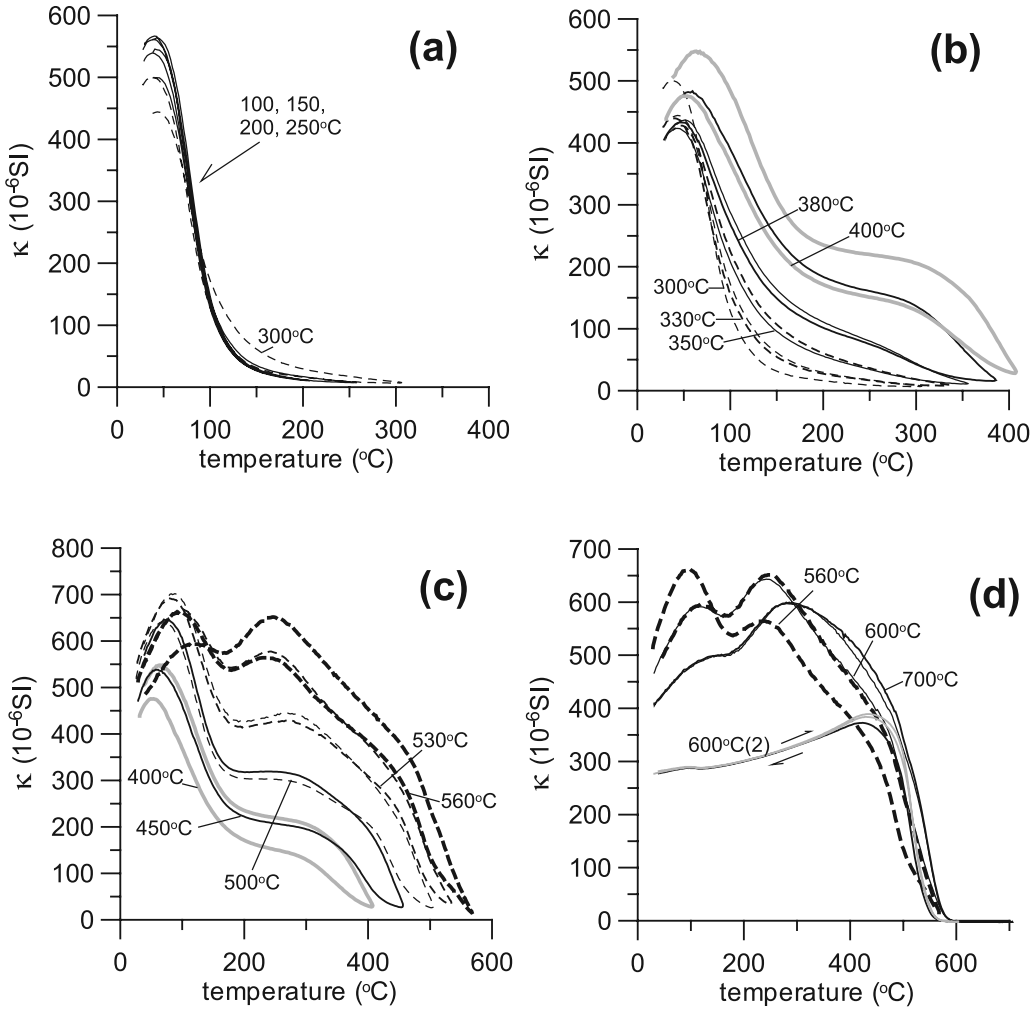

Figure 3. Temperature dependence of low-field magnetic susceptibility during stepwise heating cycles. Maximum temperature for each heating run points to its heating curve. Additional heating up to 600°C was conducted after three heating runs up to 700°C, shown in (d) as 600°C(2).

slightly above its heating curve, with a smaller susceptibility at room temperature, suggesting the start of inversion. Above 300°C treatment temperature, clear irreversibility of the heating and cooling curves suggests the formation of a higher T_c phase. With increasing treatment temperatures up to 560°C, the lower T_c phase decreases and the higher T_c phase becomes dominant (Figures 3b and 3c). The ~580°C T_c (Figure 3d) indicates that the stable newly formed magnetic phase is magnetite.

[13] The temperature dependence of magnetization was measured using a Magnetic Measurements Variable Field Translation Balance (VFTB). A fresh specimen (NLB-2) was stepwise heated in a steady DC field of 363 mT in air. Induced magnetization was measured in both heating and cooling runs. Target temperatures were set to 150, 250, 300, 350, 400, 500, 550, 600, and 700°C. The temperature sweeping rate was ~30°C min^{-1}. In the first three runs, all the heating and cooling curves are similar (Figure 4). For the first three runs, their cooling curves are below the heating curves. This could be due to the used high sweeping rate. With increasing the treatment temperatures, their cooling curves are above the heating curves, indicating a relatively strong magnetic phase with higher T_c is gradually formed. This is consistent with the $k-T$ curves although the latter shows more complexities due to effects related to grain sizes.

4.2. Hysteresis Measurements

[14] Hysteresis loops were measured on the VFTB using a maximum field of 1 T (Figure 5). The remanence coercivity (B_{cr}) was determined from back field demagnetization curves. Ratios of six fresh specimens (M_{rs}/M_s = 0.17, B_{cr}/B_c = 1.64) indicate pseudosingle-domain (PSD) grains (B_c is coercive force). After heating to 700°C, those ratios dramatically increase, shifting toward the SD region in the Day plot [*Day et al.*, 1977], and the loop shows a typical pot-bellied shape.

[15] Hysteresis loops of two specimens were measured at the designed temperature in steps of 50–100°C up to 600°C to monitor the temperature dependence of M_s and M_{rs}. Hysteresis loops change from strongly ferromagnetic (pot-bellied shape) at the room temperature to superparamagnetic at 100 and then paramagnetic at 150°C and above (Figure 5). The rapid drops in M_{rs} (Figure 6a) and M_s (Figure 6b) around 150°C mark the T_b and T_c of ATM, respectively. The

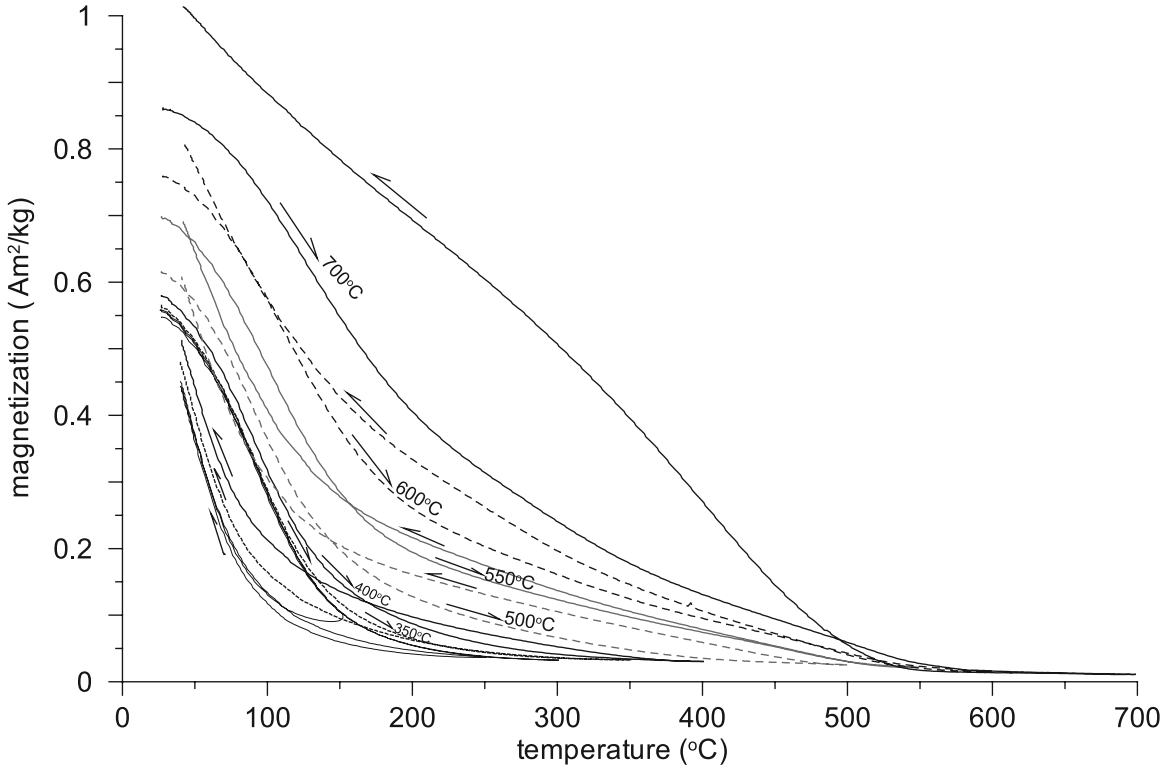

Figure 4. Stepwise thermomagnetic curves (thin lines). Specimens were heated in air in a steady field of 363 mT. Maximum heating temperatures are 150, 250, 300, 350, 400, 500, 550, 600, and 700°C.

consistency between its T_b and T_c suggests that the particle size is in coarse-grained region. Interestingly, it is noted that the M_{rs} and M_s slightly increase again above 300°C and rapidly drop to minima between 550 and 600°C. Again, this behavior suggests a formation of small amount of magnetite with a T_c of ~585°C.

[16] As seen in Figures 6c and 6d, the room temperature M_{rs}, M_s are nearly constant when the treatment temperature is below 300°C, but increase after heating to over 400°C. The coercive force of specimens are stable ($B_c \sim 7$ mT) below 600°C. B_{cr} shows a slight increase with treatment temperatures from 13 to 15 mT (not shown).

[17] Hysteresis loops and remanence coercivity measurement were also conducted at room temperature on the specimens NLB-e to h heated by the Thellier-Coe experiment (see section 3). Specimens e to h were exposed to maximum temperatures of 200, 250, 330, and 380°C, respectively. M_s and M_{rs} values are nearly constant or slightly increase, rather than decrease, through treatment temperatures over 300°C (Figures 6c and 6d).

4.3. Remanent Magnetization

[18] In order to further test possible changes of magnetization capacities by heating, we measured saturation isothermal remanent magnetization (SIRM), acquired in a pulse field of 2.7 T, and ARM, imparted in a peak AF field of 80 mT with a bias field of 50 μT, on six specimens thermally treated in the Thellier-Coe paleointensity experiment. These six specimens suffered the same thermal treatments as the specimens shown in Figures 1 and 2. They were stepwise exposed to peak temperatures of 200, 250, 330 and 380°C, respectively. SIRMs were measured on thermally treated specimens (NLB-3 to 5) and ARMs on (NLB-6 to 8). It is noted that both SIRM and ARM increased about 20 and 40 percent, respectively, with increasing treatment temperatures (Figure 7). ARM/SIRM values significantly increase after the 300°C treatment, suggesting formation of fine-grained magnetite.

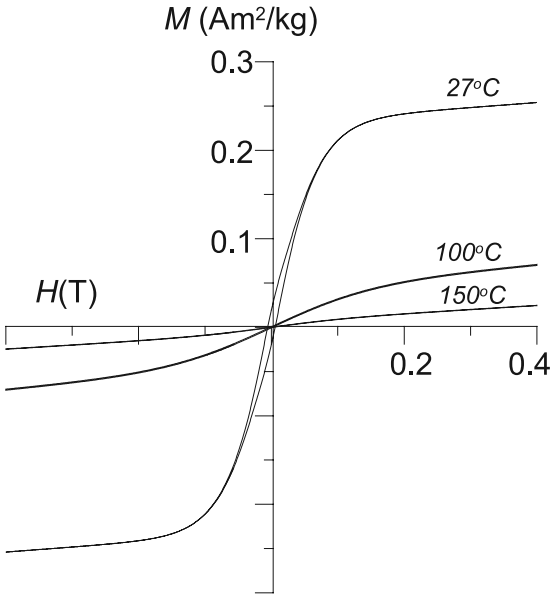

Figure 5. Hysteresis loops measured at temperatures of 27, 100, and 150°C, showing behavior ranging from ferrimagnetic to paramagnetic.

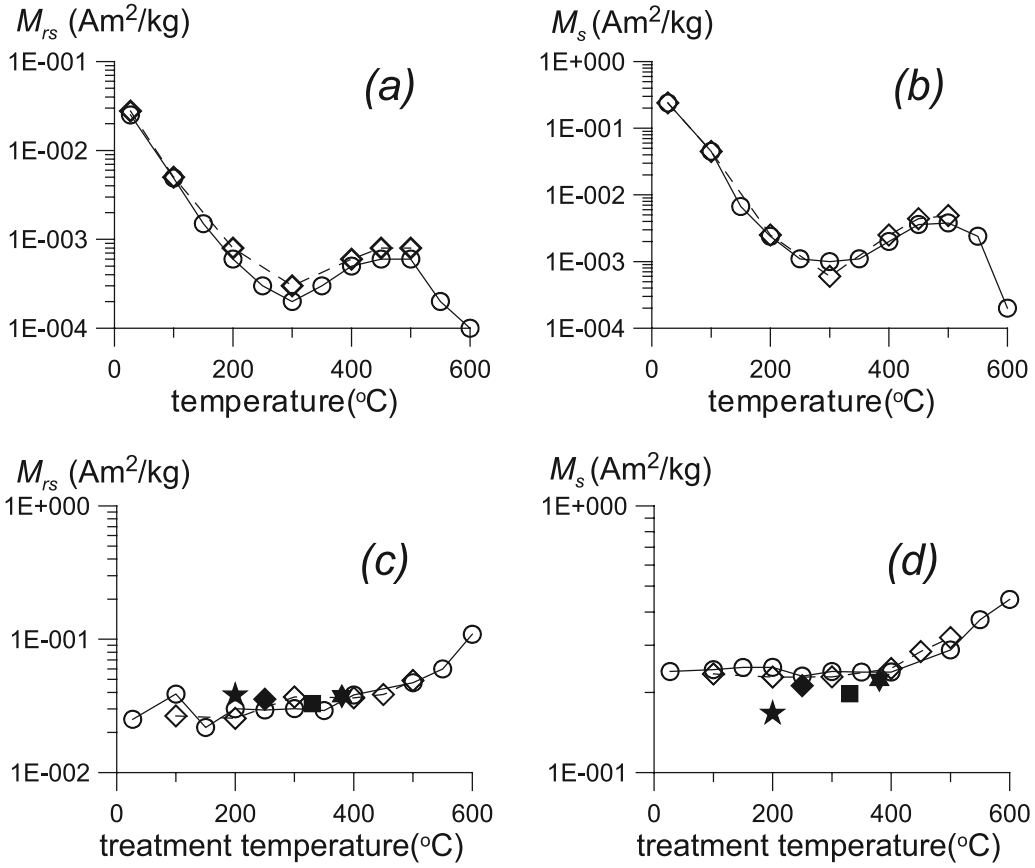

Figure 6. Remanent magnetizations determined from hysteresis loops of six specimens thermally treated at various temperatures up to 600°C. M_s and M_{rs} of two specimens (heated in air on VFTB) (open circles and diamonds) were calculated from hysteresis loops measured at both (a and b) high temperatures and (c and d) room temperatures. For comparison, M_s and M_{rs} of specimens e to h (heated in argon in the Thellier-Coe experiments exposed to maximum temperatures of 200, 250, 330, and 380°C) (solid symbols) from hysteresis loops measured at room temperatures are also shown in Figures 6c and 6d.

[19] Together, thermomagnetic curves, hysteresis, and remanent magnetization measurements demonstrate there is no obvious decrease of magnetization capacities in specimens treated above 300°C. This does not support the hypothesis that the abnormal decrease of pTRM gains above 300°C is caused by a transformation from a strongly magnetic to a weakly magnetic phase.

4.4. Behaviors of SIRM and AC Susceptibility at Low Temperature

[20] Fresh and seven stepwise heated specimens (maximum temperatures to 250, 350, 400, 450, 490, 555, and 600°C) were further studied by low-temperature magnetic measurements at the Institute for Rock Magnetism, University of Minnesota. The zero field cooling of $SIRM_{300K}$

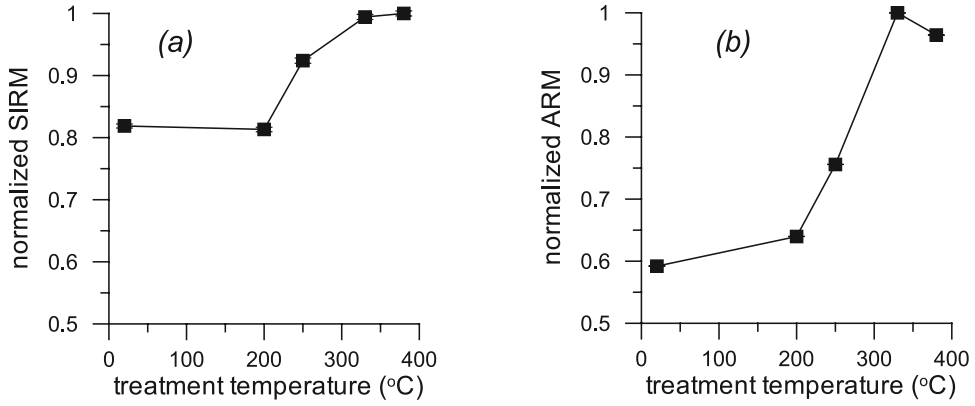

Figure 7. (a) Normalized averaged room temperature saturation isothermal remanent magnetization and (b) anhysteretic remanent magnetization of thermally treated specimens NLB-3 to 8 in the Thellier-Coe experiment. See text for details.

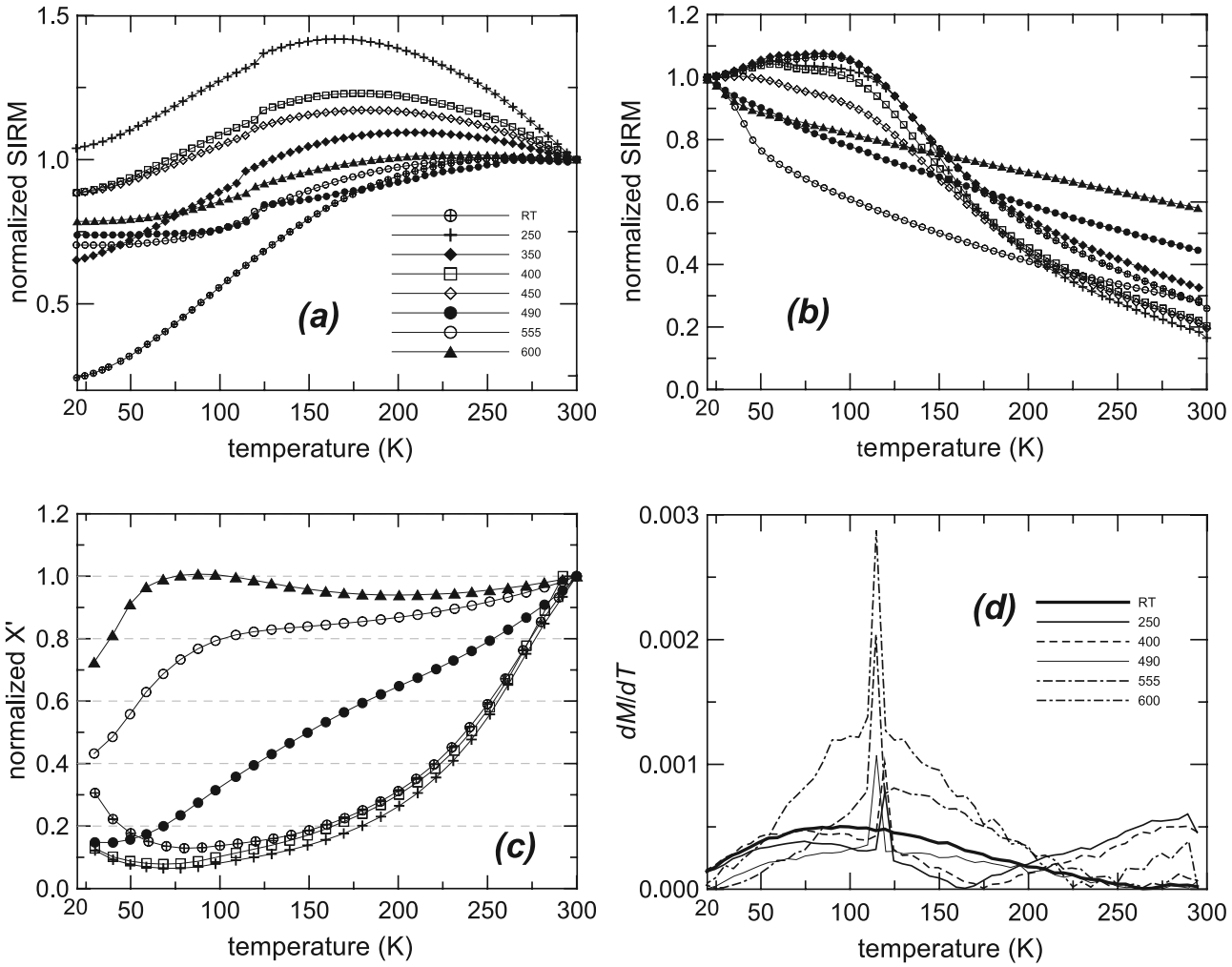

Figure 8. Low-temperature magnetic properties of unheated (RT) and stepwise heated specimens (maximum temperatures are shown). (a) Cooling of $SIRM_{300K}$ (acquired in a static field of 2.5 T at 300 K). (b) Warming of $SIRM_{20K}$ (acquired in a static field of 2.5 T at 20 K). (c) Temperature dependence of in-phase AC susceptibilities (X′), data normalized to the initial value (X'_{300K}) for each specimen. (d) Corresponding *dM*/*dT* data calculated from the curves in Figure 8a.

(acquired at 300 K at a field of 2.5 T) down to 20 K and warming of $SIRM_{20K}$ (acquired at 20 K at a field of 2.5 T) up to 300 K were conducted on the MPMS-5 Quantum Design SQUID magnetometer at temperature intervals of 5 K. Both the $SIRM_{300K}$ and $SIRM_{20K}$ values increase systematically with the thermal treatment temperatures.

[21] Figure 8a shows zero field cooling behaviors of $SIRM_{300K}$ (normalized by initial $SIRM_{300K}$). For the fresh specimen, remanence gradually decreases with temperatures down to 20 K. However, remanences of specimens thermally treated by 250, 350, 400 and 450°C increase first with temperature down to ~160 K, then decrease down to 20 K. Intensity drops around 120 K mark the Verwey transition of magnetite (Figures 8a and 8d) and confirm the neoformation of magnetite. Figure 8b shows zero field warming behaviors of $SIRM_{20K}$ (normalized by initial $SIRM_{20K}$). It shows that remanences of the fresh specimen and specimens heated after 250, 350, 400 and 450°C are stable below 100 K and decay rapidly above 100 K up to 300 K. In contrast, specimens heated after 450, 490, 555 and 600°C decay from lower temperatures and the remanence left at 300 K increased.

[22] The temperature dependence of AC susceptibility was measured on a LakeShore Cryotronics AC susceptometer measured at 10 K interval from 30 to 300 K in an AC field of 200 A m^{-1} RMS, using a frequency of 400 Hz. The warming curves of in-phase AC susceptibility from 30 to 300 K on specimens heated after 250, 350, 400, 490, 555, and 600°C are shown in Figure 8c. The curves for both unheated specimens and for those heated to 250, 350 and 400°C have concave-upward shapes, and susceptibilities increase during warming. The specimen heated to 490°C is characterized by a linear increase of susceptibility with temperature. In contrast, specimens heated to 555 and 600°C have convex curves. The in-phase susceptibility increases rapidly below 70 K and then remains flat up to 300 K. According to analysis of synthetic titanomagnetites [*Moskowitz et al.*, 1998], this pattern shown in Figure 8c

suggests gradual transformation from Ti-rich titanomagnetite into magnetite.

5. Discussion and Conclusions

[23] Electron microprobe and rock magnetic analyses have shown that PSD grain ATM ($Fe_{2.24}Ti_{0.64}Al_{0.12}O_4$) is the dominant remanence carrier of the studied Hannuoba basaltic samples. It has a T_c of ~100–150°C (Figures 2 to 6). Al^{3+} substitution may decrease the lattice parameter and lower the T_c and magnetization [*Richards et al.*, 1973; *Özdemir and Moskowitz*, 1992; *Dunlop and Özdemir*, 1997]. We interpret the observed decrease of pTRM in the temperature interval between 300 and 460°C (Figures 1 and 2) as being due to a partially self-reversed thermoremanence carried by ATM and newly formed magnetite. Note that somewhat increases of magnetization and remanence (Figures 4 and 7) do not support the interpretation of destruction of a strongly magnetic phase. In the Thellier-Coe experiment, we used a weak field with an intensity of 30 μT (0.3 Oe). The effect of field intensity can easily be excluded, because linear relationship between TRM and field in the range 0.1–1 Oe has been experimentally observed on ATM [*Özdemir and O'Reilly*, 1982; *O'Donovan et al.*, 1986]. Maghemitization of ATM induced by lengthy heating can also be ruled out, because it would reduce linearly the remanence intensities [e.g., *Brown and O'Reilly*, 1988].

[24] Thermomagnetic curves shown in Figures 3 and 4 and remanent magnetization in Figures 6c and 6d indicate that ATM is thermally stable up to about 300°C. Above 300°C, the ATM phase is gradually transformed into magnetite with a higher T_c of ~585°C (Figures 3d, 6a, and 6b). The increases of ARM and SIRM values in Figure 7 can be interpreted by two possibilities: (1) the formation of fine-particle magnetite and (2) multidomain grains of ATM acting in a SD state as noted previously by *Metcalf and Fuller* [1986]. These remanent magnetizations as well as the values of M_s and M_{rs} (Figures 6c and 6d) suggest that magnetization capacities increase, thus thermoremanences should increase with treated temperatures. The neoformation of magnetite is also evident by the low-temperature measurements on thermally treated samples, e.g., the Verwey transition appears at 120 K on the cooling curves of $SIRM_{300K}$ after thermal treatment over 250°C runs (Figure 8d). Meanwhile, we note that the Verwey transition temperature of specimens thermal treatment above 490°C shift to lower temperature, e.g., ~115 K, which suggests an increase in the degree of oxidation of magnetite. On the basis of the results of *Moskowitz et al.* [1998], the pattern of temperature dependence of AC susceptibilities (Figure 8c) also suggests that ATM was transformed to a Ti-poor phase by heating.

[25] It has long been known that self-reversal of thermoremanence could be caused by negative magnetic coupling between two phases [e.g., *Havard and Lewis*, 1965; *Tucker and O'Reilly*, 1980; *Heller and Petersen*, 1982; *Krása et al.*, 2005]. Our rock magnetic analyses indicate there are at least two magnetic phases existing in samples heated to temperatures between 300 and 500°C, e.g., the higher T_c Ti-poor phase (magnetite) and the lower T_c Ti-rich ATM phase. The former is forming while the latter remains as the major magnetic phase. Two phases could be magnetically coupled during remanence acquisition in cooling. The higher T_c phase would block magnetization first and the magnetization of this phase would interact with remanence acquired by the coupled low-T_c phase in further cooling. The phase interaction (e.g., negative magnetic couplings) may cause the observed pTRM acquisition decrease with elevated treatment temperatures. *Krása et al.* [2005] observed the influence of oxidation on the domain configuration using a magnetic force microscopy and found that the two magnetically coupled phases lead to the lower T_c phase acquiring a TRM in a direction antiparallel to the applied external magnetic field. Their numerical modeling indicated that the domain configuration is capable of causing partial and complete self-reversal due to phase coupling of the two phases. We noted that the pTRM in our specimens did not change sign through the entire experiments. The difference could be caused by several facts. Our samples contain Al impurities, with low initial oxidation states of samples, and were heated in argon atmospheres.

[26] Although the laboratory thermal inversion may not reproduce the natural process, our data have important implications for paleomagnetism and paleointensity studies using basalts containing ATM. Our experiments suggest that basaltic rocks containing low-oxidized ATM as primary remanence carriers are probably suitable for recording directions, but not for paleointensities. If the coupling phases (high- and low-T_c) are present prior to TRM acquisition, the higher-T_c phase would be magnetized first and its magnetization could lead to a reversal via interaction during further cooling. On the other hand, if the secondary interacting phases were formed after the low-T_c phase acquires TRM by low-temperature oxidation process or laboratory heating, the primary phase might be responsible for the reversal of a later phase having a high T_c. In these two cases, the magnetizations in rocks are lowered, leading to underestimation of paleointensity. Low-temperature oxidation of titanomagnetites in ocean basalts is ubiquitous [e.g., *Matzka et al.*, 2003; *Bleil and Petersen*, 1983; *Johnson et al.*, 1996]. Even though primary TRMs in rocks are fortunately preserved in rocks [e.g., *Zhou et al.*, 1999], one cannot determine the paleointensity from temperature intervals over 300°C when using the Thellier-Coe method, because magnetomineralogical inversion start. In future, microwave and low-temperature techniques should be considered.

[27] **Acknowledgments.** We thank Michael Jackson, Nikolai Petersen, and David Krása for their detailed reviews which help to improve the manuscript. This work was supported by NSFC grants 40325011 and 40221402, CAS grant KZCX3-SW-150, and a visiting fellowship of the Institute for Rock Magnetism (IRM) to Y.X.P. Q.S.L. was supported by a Marie-Curie Fellowship (IIF) funded by the European Commission, proposal 7555. The IRM is funded by the Instruments and Facilities Program, Earth Science Division, U.S. NSF, W.M. Keck Foundation, and the University of Minnesota, Twin Cities.

References

Banerjee, S. K., and J. P. Mellema (1974), A new method for the determination of paleointensity from the A.R.M. properties of rocks, *Earth Planet. Sci. Lett.*, *23*, 177–184.

Bina, M., J. C. Tanguy, V. Hoffmann, M. Prévot, E. L. Listanco, R. Keller, K. T. Fehr, A. T. Goguitchaichvili, and R. S. Punongbayan (1999), A detailed magnetic and mineralogical study of self-reversed dacitic pumices from the 1991 Pinatubo eruption (Philippines), *Geophys. J. Int.*, *138*, 159–178.

Bleil, U., and N. Petersen (1983), Variations in magnetization intensity and low-temperature titanomagnetite oxidation of ocean floor basalts, *Nature*, *301*, 384–388.

Brown, K., and W. O'Reilly (1988), The effect of low temperature oxidation on the remanence of TRM-carrying titanomagnetite $Fe_{2.4}Ti_{0.6}O_4$, *Phys. Earth Planet. Inter.*, *52*, 108–116.

Chen, S. H., S. Y. O'Reilly, X. H. Zhou, W. L. Griffin, G. H. Zhang, M. Sun, J. L. Geng, and M. Zhang (2001), Thermal and petrological structure of the lithosphere beneath Hannuoba, Sino-Korea Craton China: Evidence from xenoliths, *Lithos*, *56*, 267–301.

Coe, R. S. (1967), Palaeo-intensities of the Earth's magnetic field determined from Tertiary and Quaternary rocks, *J. Geophys. Res.*, *72*, 3247–3262.

Day, R., M. Fuller, and V. A. Schmidt (1977), Hysteresis properties of titanomagnetites: Grain size and composition dependence, *Phys. Earth Planet. Inter.*, *13*, 260–267.

Doubrovine, P. V., and J. A. Tarduno (2004), Self-reversed magnetization carried by titanomaghemite in oceanic basalts, *Earth Planet. Sci. Lett.*, *222*, 959–969.

Dunlop, D. J., and Ö. Özdemir (1997), *Rock Magnetism: Fundamentals and Frontiers*, 573 pp., Cambridge Univ. Press, New York.

Fan, Q. C., and P. R. Hooper (1991), The Cenozoic basaltic rocks of eastern China: Petrology and chemical composition, *J. Petrol.*, *32*, 765–810.

Gapeev, A. K., and S. K. Gribov (2002), Partial self-reversal of the thermoremanent magnetization created by titanomagnetites subjected to multiphase oxidation, *Izv. Phys. Solid Earth*, *38*, 713–722.

Havard, A. D., and M. Lewis (1965), Reversed partial thermo-magnetic remanence in natural and synthetic titano-magnetite, *J. R. Astron. Soc. Can.*, *10*, 59–68.

Heller, F., and N. Petersen (1982), Self-reversal explanation for the Laschamp/Olby geomagnetic field excursion, *Phys. Earth Planet. Inter.*, *30*, 358–372.

Hoffman, K. A. (1982), Partial self-reversal in basalts containing mildly low-temperature oxidized titanomagnetite, *Phys. Earth Planet. Inter.*, *30*, 357.

Johnson, H. P., D. Van Patten, and W. Sager (1996), Age-dependent variation in the magnetization of seamounts, *J. Geophys. Res.*, *101*, 13,701–13,714.

Krása, D., V. P. Scherbakov, T. Kunzmann, and N. Petersen (2005), Self-reversal of remanent magnetization in basalts due to partially oxidized titanomagnetites, *Geophys. J. Int.*, *162*, 115–136.

Matzka, J., D. Krása, T. Kunzmann, A. Schult, and N. Petersen (2003), Magnetic state of 10–40 Ma old ocean basalts and its implications for natural remanent magnetization, *Earth Planet. Sci. Lett.*, *206*, 541–553.

Metcalf, M., and M. Fuller (1986), Domain observations of titanomagnetites from room temperature to Curie point and the nature of thermoremanent magnetism in fine particles, *Nature*, *321*, 847–849.

Moskowitz, B. M., M. Jackson, and C. Kissel (1998), Low-temperature magnetic behavior of titanomagnetites, *Earth Planet. Sci. Lett.*, *157*, 141–149.

Nagata, T., S. Uyeda, and S. Akimoto (1952), Self-reversal of thermoremanent magnetization of igneous rocks, *J. Geomagn. Geoelectr.*, *4*, 22–38.

Néel, L. (1951), L'inversion de l'aimantation permanente des roches, *Ann. Geophys.*, *7*, 90–102.

O'Donovan, J. B., D. Facey, and W. O'Reilly (1986), The magnetization process in titanomagnetite ($Fe_{2.4}Ti_{0.6}O_4$)in the 1–30 μm particle size, *Geophys. J. R. Astron. Soc.*, *87*, 897–916.

O'Reilly, W., and S. K. Banerjee (1966), Oxidation of titanomagnetites and self-reversal, *Nature*, *211*, 26–28.

Özdemir, Ö., and B. M. Moskowitz (1992), Magnetostriction in aluminum-substituted titanomagnetites, *Geophys. Res. Lett.*, *12*, 2361–2364.

Özdemir, Ö., and W. O'Reilly (1982), An experimental study of the intensity and stability of thermoremanent magnetization acquired by synthetic monodomain titanomagnetite substituted by aluminum, *Geophys. J. R. Astron. Soc.*, *70*, 141–154.

Pan, Y. X., M. J. Hill, and R. X. Zhu (2005), Paleomagnetic and paleointensity study of an Oligocene-Miocene lava sequence from the Hannuoba basalts in northern China, *Phys. Earth Planet. Inter.*, *151*, 21–35.

Prévot, M., E. A. Mankinen, R. S. Coe, and C. S. Gromme (1985), The Steens Mountain (Oregon) geomagnetic polarity transition: 2. Field intensity variations and discussion of reversal models, *J. Geophys. Res.*, *90*, 10,417–10,448.

Richards, J. C. W., J. B. O'Donovan, Z. Hauptman, W. O'Reilly, and K. M. Creer (1973), A magnetic study of titanomagnetite substituted by magnesium and aluminum, *Phys. Earth Planet. Inter.*, *7*, 437–444.

Schult, A. (1968), Self-reversal of magnetization and chemical composition of titanomagnetites in basalts, *Earth Planet. Sci. Lett.*, *4*, 57–63.

Thellier, E., and O. Thellier (1959), Sur l'intensité du champ magnétique terrestre le passé historique et géologique, *Ann. Geophys.*, *15*, 285–376.

Tian, L. L., R. X. Zhu, and Y. X. Pan (2002), Rock-magnetic properties of Hannuoba basalt in Zhangbei section, *Chin. J. Geophys.*, *45*, 832–838.

Tucker, P., and W. O'Reilly (1980), Reversed thermoremanent magnetization in synthetic titanomagnetites as a consequence of high temperature oxidation, *J. Geomagn. Geoelectr.*, *32*, 341–355.

Verhoogen, J. (1956), Ionic reordering and self-reversal of magnetization in impure magnetites, *J. Geophys. Res.*, *61*, 201–209.

Yu, Y. J., D. J. Dunlop, and Ö. Özdemir (2003), Are ARM and TRM analogs?, *Earth Planet. Sci. Lett.*, *205*, 325–336.

Zheng, Z., H. Tanaka, Y. Tatumi, and M. Kono (2002), Basalt platforms in Inner Mongolia and Hebei Province, northeastern China: New K–Ar ages, geochemistries, and revision of palaeomagnetic results, *Geophys. J. Int.*, *151*, 654–662.

Zhi, X. C., Y. Song, F. A. Frey, J. Feng, and M. Z. Zhai (1990), Geochemistry of Hannuoba basalts, Eastern China; constraints on the origin of continental alkalic and tholeiitic basalt, *Chem. Geol.*, *88*, 1–33.

Zhou, W., R. Van der Voo, and D. R. Peacor (1999), Preservation of pristine titanomagnetite in older ocean-floor basalts and its significance for paleointensity studies, *Geology*, *27*, 1043–1046.

Zhu, R., C. Shi, and Q. Liu (2003), Anisotropy of magnetic susceptibility of Hannuoba basalt, northern China: Constraints on the vent position of the lava sequences, *Geophys. Res. Lett.*, *30*(2), 1066, doi:10.1029/2002GL016215.

C. Deng, Y. Pan, H. Qin, and R. Zhu, Paleomagnetism and Geochronology Laboratory (SKL-LE), Institute of Geology and Geophysics, Chinese Academy of Sciences, Beijing 100029, China. (yxpan@mail.iggcas.ac.cn)

Q. Liu, National Oceanography Centre, University of Southampton, European Way, Southampton SO14 3ZH, UK.